NBSIR 76-1031

Shape Dependence of Light-Scattering Behavior of Dust Particles

R. Zerull

Ruhr University
Bochum-Querenburg
West Germany

Translated for:

Center for Fire Research
Institute for Applied Technology
National Bureau of Standards
Washington, D. C. 20234

June 1976

Final Report

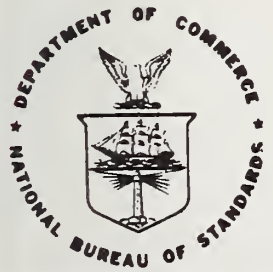

U S. DEPARTMENT OF COMMERCE
NATIONAL BUREAU OF STANDARDS

NBSIR 76-1031

SHAPE DEPENDENCE OF LIGHT-SCATTERING BEHAVIOR OF DUST PARTICLES

R. Zerull

Ruhr University
Bochum-Querenburg
West Germany

Translated for:

Center for Fire Research
Institute for Applied Technology
National Bureau of Standards
Washington, D. C. 20234

June 1976

Final Report

U.S. DEPARTMENT OF COMMERCE, Elliot L. Richardson, *Secretary*
James A. Baker, III, *Under Secretary*
Dr. Betsy Ancker-Johnson, *Assistant Secretary for Science and Technology*

NATIONAL BUREAU OF STANDARDS, Ernest Ambler, *Acting Director*

PREFACE

This report is a translation of paper prepared by Dr. R. Zerull and presented by him at the Colloquium on Aerosol Measurement Techniques, March 4, 1975, in Aachen, West Germany. The Colloquium was presented by the Institute for Electronics Communication Technology of the Rheinish-Westfalian Technical College, Aachen, in conjunction with the Gesamthochschule in Duisburg.

This translation has been prepared to disseminate useful information to interested fire research personnel on a need-to-know basis and is not an original work of the Center for Fire Research.

We express our appreciation to the author, Dr. R. Zerull, for his permission and assistance in making this information available.

We also express our appreciation to the Joint Publication Research Service, Arlington, Virginia, who provided the translation of the original paper.

Richard G. Bright
Program for Fire Detection
and Control Systems
Center for Fire Research

CONTENTS

LIST OF FIGURES

SHAPE DEPENDENCE OF LIGHT-SCATTERING BEHAVIOR OF DUST PARTICLES

R. Zerull

Abstract

The most important characteristics which determine the light-scattering behavior of particles is their size distribution, their concentration, their shape, and their material composition. This paper concerns itself with the measurement of the effects of shape on light-scattering behavior. Only a few shapes have been appropriately modeled and if the shape dependence can be determined, the remaining characteristics pose no special difficulties.

Key words: Aerosols; dusts; light-scattering; Mie theory; particles; Rayleigh scattering.

1. INTRODUCTION

Problems connected with light-scattering from dust particles can roughly be divided into two categories. In one case, the scattering characteristics of a known particle system are calculated or measured. The second case is the inverse problem; here, conclusions are drawn from measured scattered light with respect to the composition of the particles producing it. The most important distinguishing characteristics, on which the scattering behavior characteristically depends here, are the material, the form, the size distribution, and the spatial distribution of the particles. To be able to associate the measured light-scattering characteristics as unambiguously as possible with a definite particle system, it is therefore necessary to know as accurately as possible the influences of the cited distinguishing parameters on the scattering behavior. Appropriate model calculations have hitherto been possible only for a few special particle shapes, such as, for example, spheres, layered spheres, and infinitely-long circular cylinders, whereby variation of the remaining parameters does then indeed pose no special difficulties. For this reason, measurement of the shape dependence of the scattered radiation shall occupy the foreground in the present paper.

2. COMPUTATIONAL FORMULATION OF A SCATTERING PROCESS

The physical characteristics of the particles are described by the complex index of refraction $m = m' - jm''$. The generally customary size parameter α = circumference/wavelength, which is derived from a sphere, is to be used here to specify the size of a particle.

Figure 1 shows the geometry of a scattering process. The light source, the scattering body, and the observer who records the scattered light at a scattering angle θ, span the so-called scattering plane.

If the scattering process is separately considered for the two directions of polarization, vertical (Index 1) and parallel (Index 2) to the scattering plane, the following relation [1][1] is obtained between the intensities recorded at the site of the scattering body (Index 0) and the scattering intensity (Index s), recorded at a distance r from the scattering body at an angle θ referred to a fixed plane:

$$I_{s1}(\theta) = \frac{\lambda^2}{4\pi^2 r^2} \cdot i_1(\theta) \cdot I_{o1} \quad (\lambda = \text{Wellenlänge})$$

$$I_{s2}(\theta) = \frac{\lambda^2}{4\pi^2 r^2} \cdot i_2(\theta) \cdot I_{o2}.$$

In this representation, the scattered radiation is characterized by the scattering functions i_1 and i_2, which depend on the characteristics of the scattering body and on the scattering angle θ, but not on the distance of observation r. Their calculation and measurement will be discussed in the following sections.

With this scattering function, the generally customary degree of linear polarization

$$P = \frac{i_1 - i_2}{i_1 + i_2} = \frac{i_1 - i_2}{i}$$

can be defined. If the incident radiation consists of natural, i.e. unpolarized, light of intensity I_o, the given formalism is exact for spherical particles. For other particles,

[1] Numbers in brackets refer to the literature references listed at the end of this paper.

it is often valid to a good approximation if one sets $I_{o1} = I_{o2} = I_o/2$ [2].

All these considerations are first of all valid for an individual particle in a definite spatial orientation. If there are several particles, a "resultant scattering function" is obtained by simple addition of the individual scattering functions. It is here presupposed, of course, that the particles are sufficiently distant from one another so that the scattered radiation of neighboring particles is negligible compared to the intensity of the primary light source; thus no significant multiple scattering occurs. When several particles are considered, a distinction is made between monodisperse mixtures (all particles the same size, with statistical orientation) and polydisperse mixtures (particles in a prescribed size distribution and with statistical orientation).

If the just-mentioned "resultant scattering function" of a mixture of particles is divided by the number of particles the so-called "averaged scattering function" is obtained. It can be associated with a fictitious particle, which represents the scattering characteristics of a whole mixture. In the further discussion, the average scattering functions of monodisperse mixtures will be designated by $\bar{i}$, those of polydisperse mixtures by σ. The situation becomes somewhat more complicated when the particles of a mixture occupy such a large space that different scattering angles are obtained with respect to the observer and the light source. In this case, the scattering intensities originating from individual particles must be added taking into account the different scattering angles.

3. DETERMINATION OF SCATTERING FUNCTIONS

3.1. Calculation of Scattering Functions

In this section various possibilities are sketched for computational determination of the scattering functions. First of all two approximations will be mentioned [1]. Particles whose dimensions are very small compared to the wavelength, behave approximately like electric dipoles. Qualitatively, a scattering diagram thus results as is shown in figure 2.

The scattering behavior of particles, whose dimensions are large compared to the wavelength of the incident radiation, can be approximately described by geometric optics. Here, the scattering diagram is composed of the diffraction diagram, determined from the Fraunhofer formulas (independent of material) according to the current cross section, and

a portion to be calculated from the Fresnel formulas for reflection and refraction. This becomes clear by following a ray in figure 3.

The incident ray 1 is partly reflected (2) and partly refracted. If the refracted ray (3) again strikes the boundary of a body, it is also partially reflected and refracted (ray 4 and 5). From the summation of the outward penetrating rays, there then results the second portion required for composing the scattering diagram. This procedure is indeed quite perspicuous, but in all quite cumbersome, and furthermore inaccurate for particle sizes below $\alpha = 400$. Nevertheless, all scattering phenomena produced by water droplets (e.g. increased back scattering, rainbows) can be qualitatively explained in this fashion. Geometric optics becomes particularly simple when the material of the scattering body is so strongly absorbing that ray 3 is almost completely attenuated in its path, and thus only ray 2 needs to be considered.

Since light involves electromagnetic waves, a scattering process is exactly described by Maxwell's equations. But solutions for these, until now, exist only for a few cases, for which the boundary conditions at the boundary surfaces can be formulated particularly simply. An important special case is the sphere, for which the solution is known as "Mie Theory" [1]. This solution makes it possible, with modern computers, to determine the scattering function of nearly arbitrarily large spheres, and thus also of mixtures of spheres. Considering once again all hitherto cited possibilities for calculating scattering functions, the gap is immediately apparent, which cannot presently be closed with computationally tolerable effort. These are the scattering calculations for all non-spherical particles, which are neither very small nor very large compared to the wavelength. Although it is not, in principle, impossible to determine the scattering functions of complicated particles, the problem can still be, at this time, more easily solved experimentally, especially when one considers that the scattering behavior of mixtures of particles with various sizes and different orientations are usually the ones of interest. We thus arrive at the central theme of this paper, namely, the measurement of scattering functions.

3.2. Measurement of Scattering Function

The most obvious possibility is to measure the scattering characteristics of particles of interest directly in the optical domain. The advantage of such measurements lies in the fact that scattering functions of mixtures can be determined in a short time. But it is here difficult to give the

individual particles a definite shape as well as to simulate prescribed size distributions.

Another possibility for measuring scattering functions consists in the microwave analog experiment. Here the length of light waves and the particle size are multiplied by the same factor (order of magnitude 10^4), whereby the microwave region is attained and the particles take on convenient dimensions. In the microwave range, the same classical electromagnetic laws hold as in the optical range. Of course, for the microwave experiments, one cannot use the same material of which the particles consist that are of interest for optical applications, since the index of refraction is often already strongly frequency-dependent within small intervals. (This is even more so when the frequency differences amount to 4 powers of ten.) Accordingly, a material must be selected for the experiments which has a value in the microwave range that is of interest for optical problems. An apparatus for performing microwave analogy experiments is located in the extraterrestrial physics branch at the Ruhr University Bochum. Its technical conception will be described in the following section.

3.3. Experimental Setup

Figure 4 shows a section of the scattering chamber with the essential parts of the mechanical setup. Antennas are affixed to the columns. The transmission antenna (right in the picture) is fixed, while the receiving antenna (left in the picture) can be moved on a rail about the scattering body, which can be seen approximately in the middle of the picture. The scattering body is suspended by four nylon threads, of which two at a time are tensioned by stepping motors on the ceiling and on the floor. Various orientations of the scattering body can thus be set. The threads are so thin that they are really "invisible" to the microwaves.

The entire scattering chamber and the mechanical setup are draped with absorbing material to keep reflections at a low level.

Figure 5 shows the principal circuit diagram for the transmission-receiving, and data-sensing component. A reflex klystron serves as transmitter. It operates at a frequency of 35 GHz (K_a-band) and has a power of 250 mW. The power is led through a waveguide transmission antenna (a pyramid horn). The intensity scattered by the scattering body at a certain angle θ is received by a horn antenna of similar construction, and is brought to a diode mixing receiver. The intermediate frequency generated in association with auxiliary oscillator

I is 30 MHz. A stabilizing device maintains the transmitter and the auxiliary oscillator I always at this frequency interval. After selective amplication, the intermediate frequency signal is transposed into the low frequency range (1 KHz) by means of an auxiliary oscillator II and a broad band multiplier. Then, it is again amplified selectively and rectified. If the auxiliary oscillators are correctly adjusted, the signal that is now present is proportional to the received signal over a power range of more than 4 powers of ten. Various noise signals are present on the desired scattering signal of the test body. For one, there are reflections from the walls and from parts of the setup, which cannot be fully avoided even with absorbing covers. More critical are signals which find their way directly from the transmission to the receiving antenna. Their intensity, especially in the range of forward scattering, can exceed that of the useful signal by several orders of magnitude. All these undesired signals are present even when no scattering body is located in the field; this offers the possibility of eliminating them by adding a signal of equal amplitude but opposite phase. For this purpose, part of the transmitted energy is branched-off into the compensation circuit, where the required signal is adjusted by an attenuator and a phase shifter, and can be superimposed on the received signal by means of a "magic T." After zero equalization has been achieved, the scattering body is brought into the field, whose desired scattering signal can now be recorded without error. Compensation of the noise level must, of course, be executed anew for each scattering angle.

The required measurement time must be kept within economical limits, considering the many necessary individual measurements. For this purpose, the course of measurement has been substantially automated. Furthermore, the possibility was provided of obtaining averaged scatter functions by a direct route. As already mentioned, a signal proportional to the desired scattering signal is available at the rectifier. The subsequent integrator makes possible direct measurement of the scattering function, averaged over exactly one rotation of a rapidly-rotating scattering body. Such a measured value is available in 1-3 seconds, independent of the rotational velocity. Values measured by the digital voltmeter are stored on paper tape for further processing in the computer. The computer must first convert the recorded scattering signals into associated values of the scattering function. The required calibration factor results from comparing the measured scattering diagram with that of a calibration sphere calculated according to the Mie theory.

4. RESULTS OF MEASUREMENT

4.1. Isometric Bodies

Since only sparse results were available concerning the scattering behavior of non-spherical shapes particles, it seemed sensible in the measurements to systematically delimit it with respect to spheres, by choosing special particle shapes. Figure 6 shows several of the bodies measured at this time — first cubes and octahedrons, as regular shapes, then rough spheres, and finally irregular bodies, which are bounded by flat or concave surface sections.

Several typical results will be selected in the following discussion. They will always be juxtaposed on the Mie calculations, whereby equal volumes serve as the basis for comparison. For polydisperse mixtures, a size distribution is assumed according to the power law

$$n\, d\alpha \sim \alpha^{-K} d\alpha;$$

of course, microwave analogy experiments offer precisely the possibility of also simulating substantially more specialized distributions [2]. For economic reasons, the steps in body size had to be chosen relatively coarsely — each individual scattering body is therefore representative for a relatively large size interval. To show that no errors arise therefrom, curves have also been drawn in several of the diagrams, which result from equally coarse steps in the comparison spheres.

4.1.1. Rough Spheres

The measured spheres had a roughness of about 1/10 wavelengths. The deviation in scattering behavior relative to smooth spheres was so low, for monodisperse as well as for polydisperse mixtures, that graphic representation will here be dispensed with [2]. In particular, the rise in the back scattering range, typical for mixtures of dielectric spheres, was fully preserved.

4.1.2. Cubes

Figures 7-9 show the scattering behavior of polydisperse mixtures of cubes. Figure 7 illustrates the basic differences with respect to spheres: while the diffraction peak is preserved, essentially isotropic scattering behavior results for larger scattering angles; the intensity and the mean angular ranges lie almost one order of magnitude above that

of the comparable mixtures of spheres, while the rise in back scattering, which is typical for the latter, is absent. The polarization behavior of these cubes is neutral in the middle, whereas, by contrast, the corresponding mixtures of dielectric spheres clearly polarize negatively in this size interval. The mixture of cubes in figure 7 was divided into "smaller" and "larger" cubes for figures 8 and 9. It thus becomes clear that the larger cubes are in the first place responsible for the different course of intensity in figure 7, while small as well as large cubes contribute to the differences in the polarization behavior.

4.1.3. Octahedrons

The scattering behavior of octahedrons can be delimited with respect to spheres in the same manner as that of cubes. Indeed, the increase in intensity in the medium ranges of scattering angles turns out to be weaker [2]. This is made clear in figure 10, where monodisperse mixtures of octahedrons, cubes, and spheres are compared with one another.

4.1.4. Irregular Bodies

The irregular bodies used for the measurements deviated from spherical shape in a definite fashion: One series had 10-15 flat surface sections as a boundary ("convex bodies"), while the examples of the other series, which were always of equal volume, were bounded by concave spherical or cylindrical surface sections ("concave bodies").

In figure 11, for example, the scattering functions of polydisperse mixtures of the convex and concave bodies, as well as of equivalent spheres, are juxtaposed one on another. The size interval considered is $5.87 \leq \alpha \leq 17.79$. It is conspicuous in the diagrams that the diffraction peak, to the extent that it could be measured, is nearly identical for the irregular bodies and the mixture of spheres. For larger scattering angles, by contrast, ($\theta \geq 20°$), the courses of the curves deviate strongly from one another. The intensity in the middle range of angles is far higher with the irregular bodies than with the mixture of spheres (maximally by a factor of 5), whereby the scattering intensity of the concave bodies still lies clearly above that of the convex ones. The increase in intensity is clearer for σ_1 than for σ_2.

Since a mixture of dielectric spheres of the size order under consideration polarizes predominantly negatively, this fact indicates a neutral polarization behavior of the irregular bodies. A clear difference in the three courses of

curves can furthermore be recognized in the range of back scattering: in contrast to the strong rise in back scattering, typical for mixtures of dielectric spheres, the convex bodies here exhibit only a small rise, while the concave bodies scatter nearly isotropically in this range.

4.2. Finite Cylinders

The first exact solution of a scattering problem was found by Rayleigh in 1881 for perpendicular incident radiation on an infinitely long circular cylinder. The formalism for this is as follows [3]

$$I_{s1}(\theta) = \frac{\lambda}{\pi^2 r} \left| T_1(\theta) \right|^2 \cdot I_{o1}$$

$$I_{s2}(\theta) = \frac{\lambda}{\pi^2 r} \left| T_2(\theta) \right|^2 \cdot I_{o2}$$

$\left|T_{1,2}\right|^2$ are the cylinder scattering functions which are to be calculated. With the cylindrical scattering problem, the scattering intensity declines like 1/r. With the transition to finite cylinders of length l, the scattering formula cited in section 2 is again valid, if the observation distance is sufficiently large ($r >> \ell^2/\lambda$). With the aid of the measurements described below, it is now to be ascertained what connection exists between the cylinder scattering functions $\left|T_{1,2}(\theta)\right|^2$, which are to be calculated, and the scattering functions $i_{1,2}$ of finite circular cylinders, and to what extent this connection remains intact with the transition to non-circular cross sections. Altogether, 27 different cylinders were measured: 3 different cross sections (circular, hexagonal, square) and in each case 3 different thicknesses and lengths. The representation of the measured results in diagram form would exceed the bounds of this paper, so that here only a capsule-form summary of the results can be given:

- The best possible agreement for different cross sectional <u>shapes</u> results with equal cross sectional <u>surface</u>.
- Agreement with theory is very good for the longest ($\ell/\lambda = 8$) circular cylinders of all thicknesses for both directions of polarization; maxima and minima occur at the same scattering angles and have nearly the same values.

- The longest cylinders with non-circular cross sections still have good agreement, though, of course, the maxima and minima are less vivid, through the averaging over various orientations.

- Agreement becomes worse with decreasing length, especially for greater thicknesses. If the bodies attain isometric dimensions (length = thickness), a resemblance can be recognized only for scattering angles $\theta < 90°$.

5. CONCLUSIONS

Based on measurements performed at this time, the consequence appears that calculations with the Mie theory cannot be performed carelessly, when the particles in question are not really spherical. Only small roughnesses in spheres did not have significant influence on the scattering diagram. With all other body shapes, aggreement with the Mie theory could be determined only in the range of forward scattering.

The assertions refer in the first place only to nearly pure dielectric bodies. Investigations concerning the shape dependence of scattered radiation with strongly absorbing materials are in preparation. Furthermore, a closer investigation must be made concerning which body shapes still entail increased back scattering. And finally, another interesting measurement problem is represented by nonhomogeneous bodies, for example loose conglomerates of materials.

6. REFERENCES

[1] Kerker, M., The Scattering of Light and Other Electromagnetic Radiation, Academic Press, New York (1969).

[2] Zerull, R., Microwave Analogy Experiments for Light Scattering from Dust Particles, BMFT-FB W73-18 (1973).

[3] Hulst, H. C. van de, Light Scattering by Small Particles, John Wiley, New York (1957).

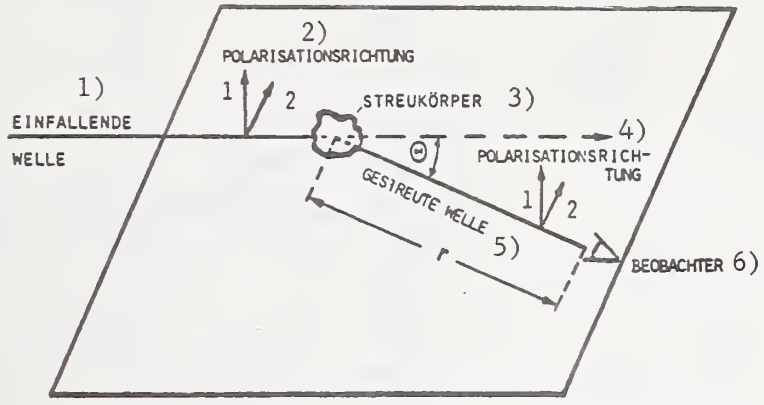

Figure 1. Geometry of a Scattering Process

1. Incident Wave
2. Direction of Polarization
3. Scattering Body
4. Direction of Polarization
5. Scattered Wave
6. Observer

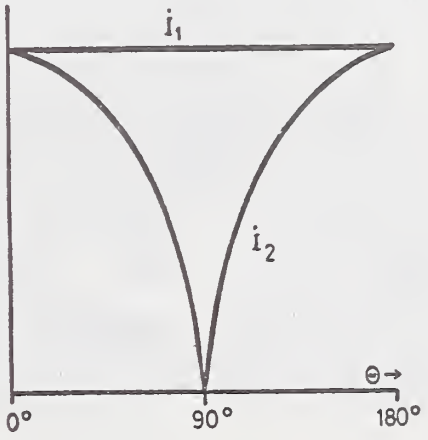

Figure 2. Rayleigh Scattering

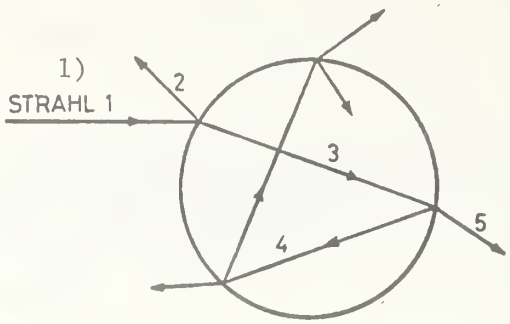

Figure 3. Geometric Optics
1. RAY 1

Figure 4. Microwave Scattering System

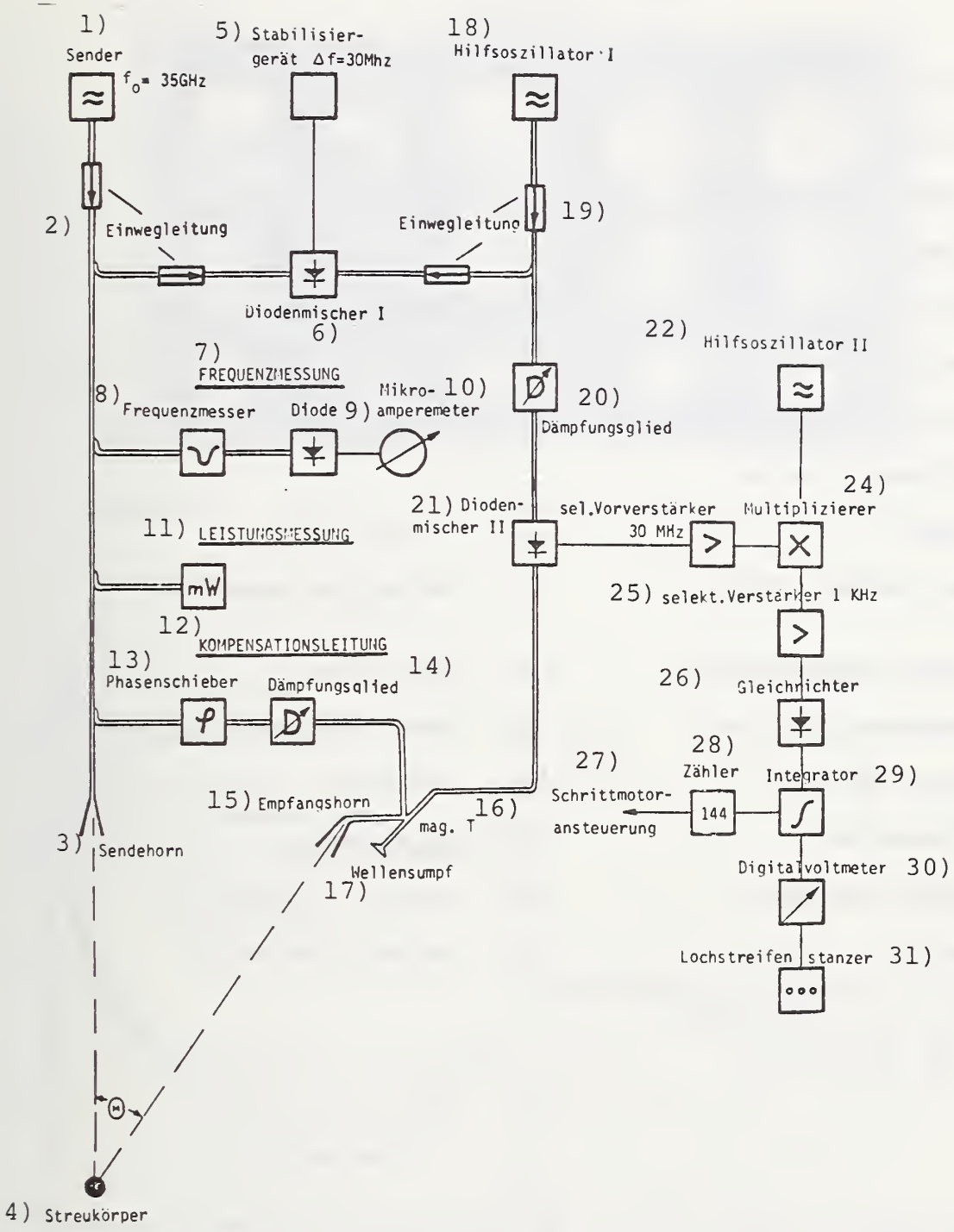

Figure 5. Principal Circuit Diagram of the Microwave Scattering System (See Key on next page)

KEY (to Figure 5)

1. Transmitter
2. Isolator
3. Transmission Horn
4. Scattering Body
5. Stabilizing Device
6. Diode Mixer I
7. Frequency Measurement
8. Frequency Meter
9. Diode
10. Mocroampere Meter
11. Power Measurement
12. Compensation Line
13. Phase Shifter
14. Attenuator
15. Receiving Horn
16. Magic T
17. Termination
18. Auxiliary Oscillator I
19. Isolator
20. Attenuator
21. Diode Mixer II
22. Auxiliary Oscillator II
23. Selective Preamplifier 30 MHz
24. Multiplier
25. Selective Amplifier 1 KHz
26. Rectifier
27. Stepping Motor Control
28. Counter
29. Integrator
30. Digital Voltmeter
31. Paper Tape Punch

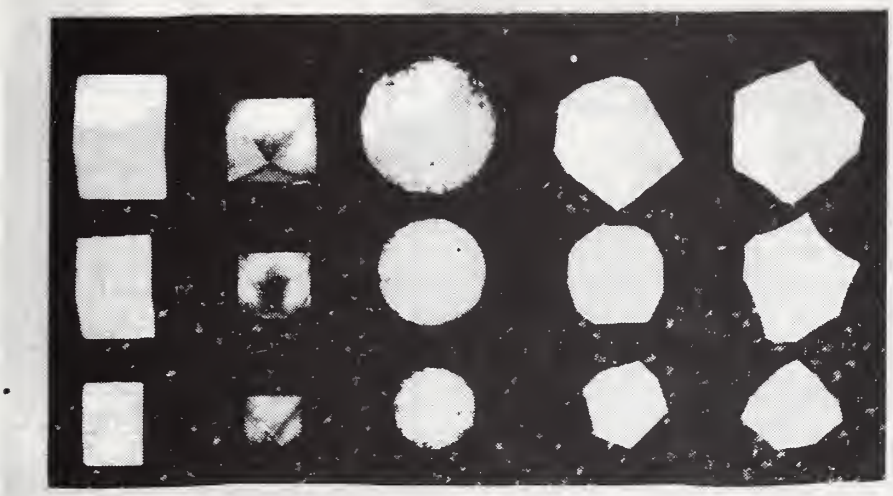

Figure 6. Part of the Measured Scattering Bodies

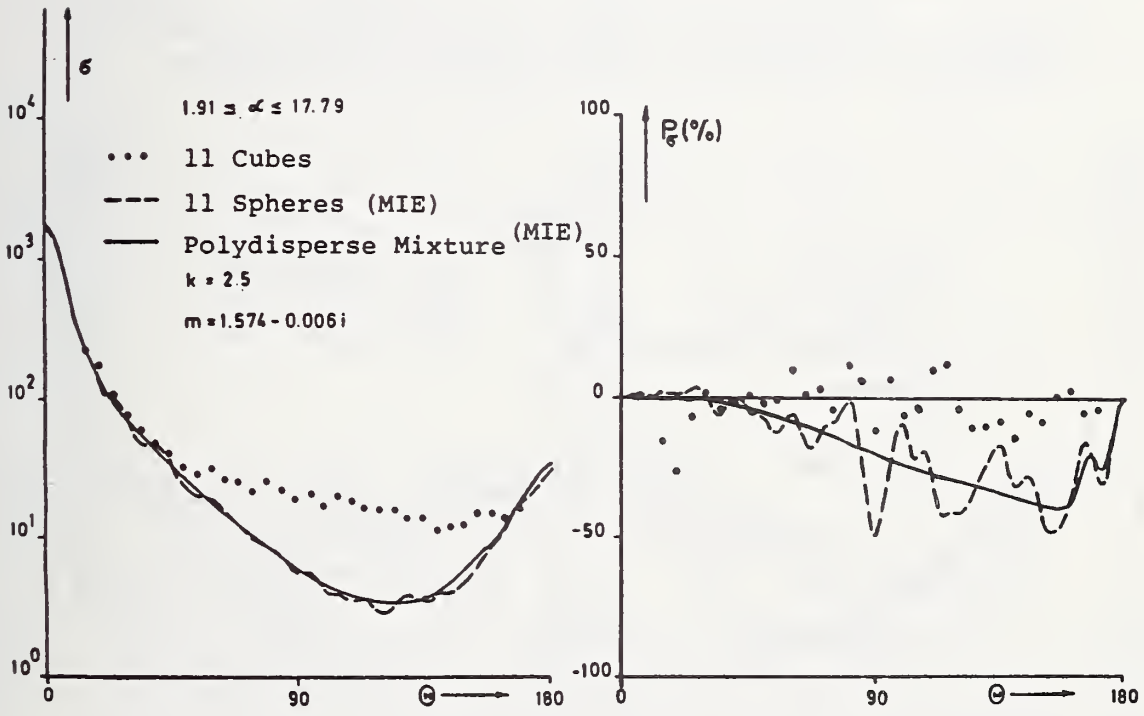

Figure 7. Scattering Behavior for a Polydisperse Mixture of Cubes Compared to Spheres

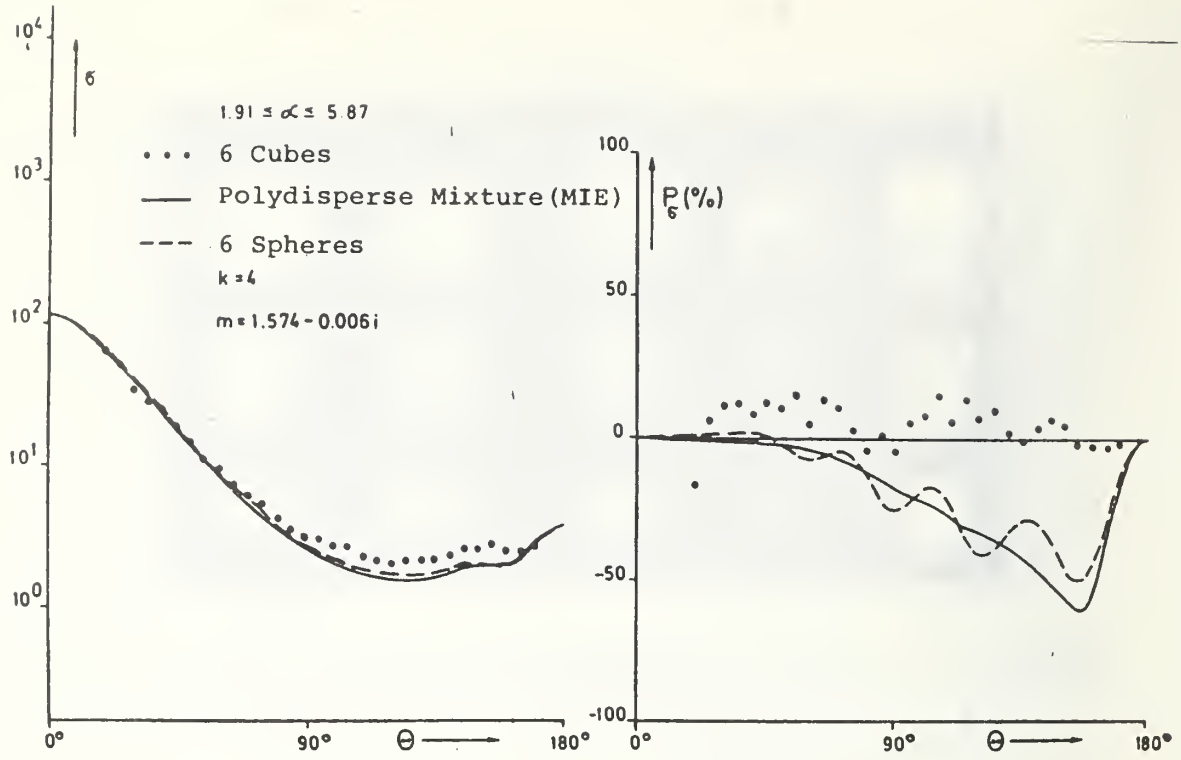

Figure 8. Scattering Behavior for a Polydisperse Mixture of "Smaller" Cubes Compared to Spheres

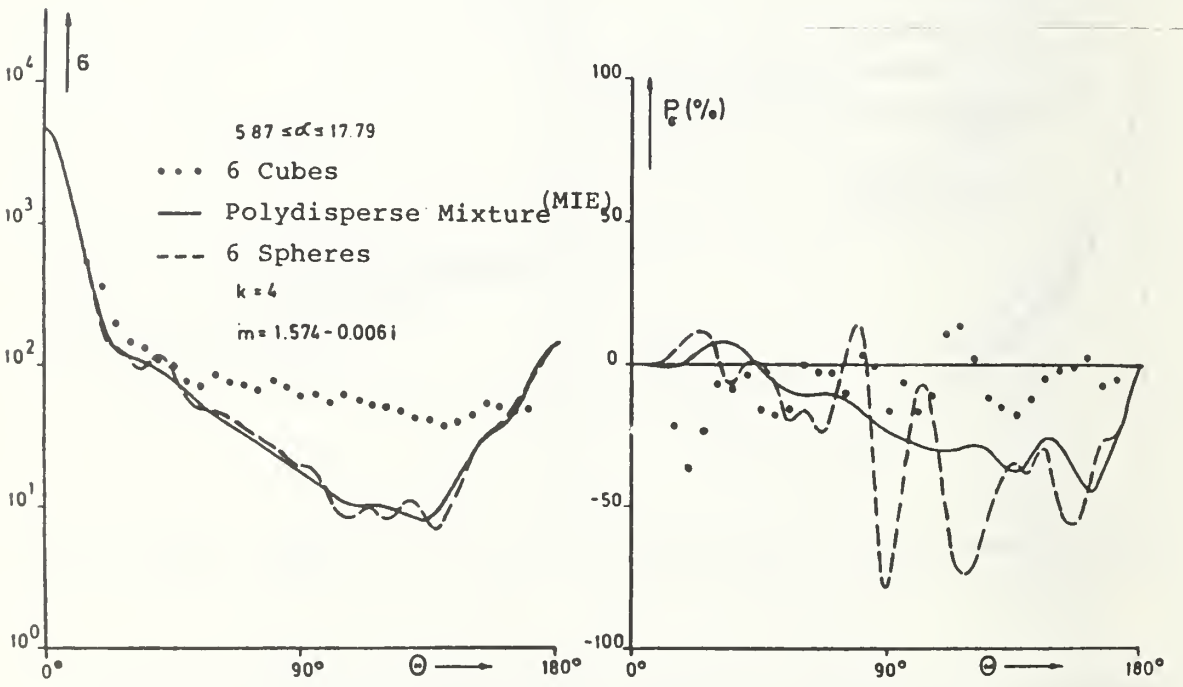

Figure 9. Scattering Behavior for a Polydisperse Mixture of "Larger" Cubes Compared to Spheres

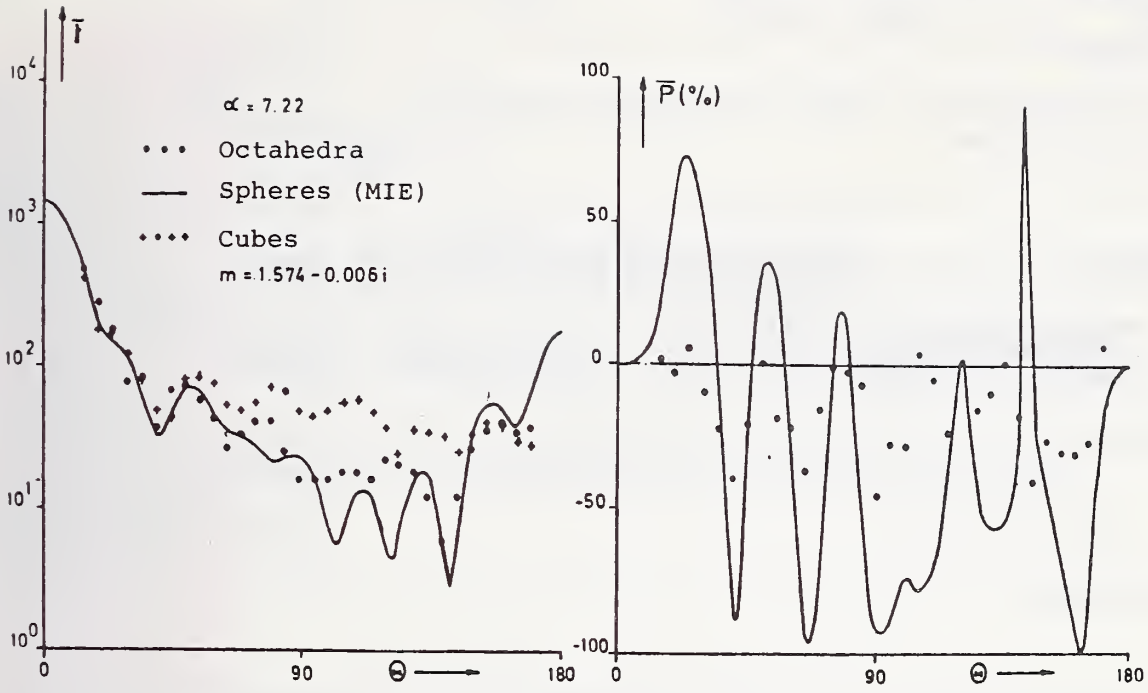

Figure 10. Scattering Behavior for a Monodisperse Mixture of Octahedrons, Cubes and Spheres

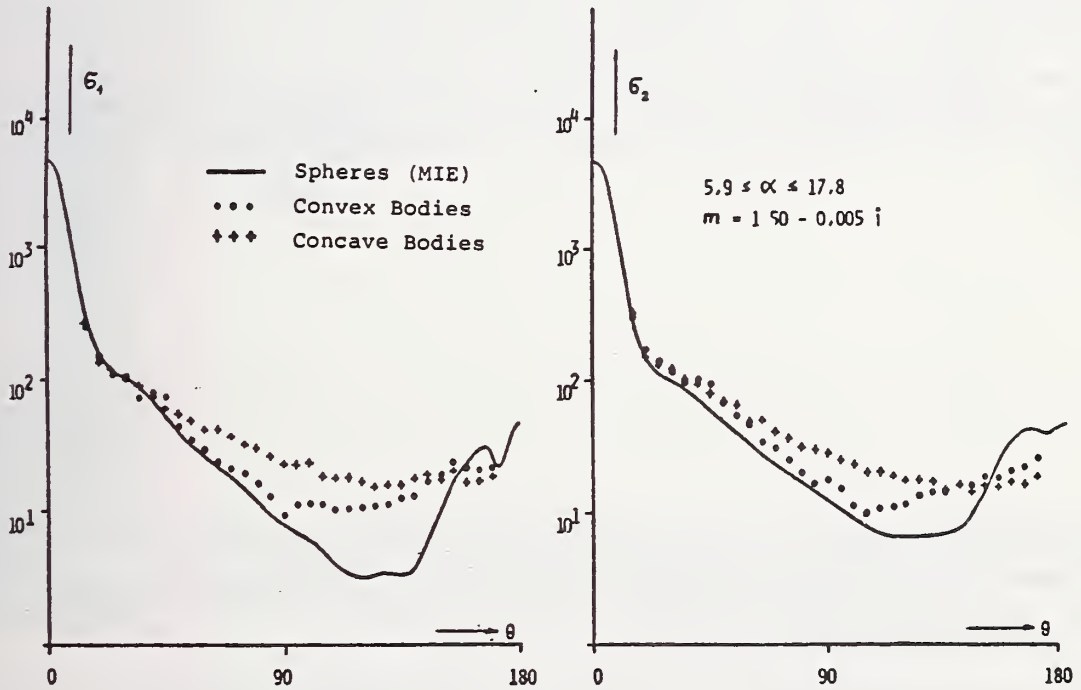

Figure 11. Scattering Behavior for a Polydisperse Mixture of Convex and Concave Bodies Compared to Spheres

NBS-114A (REV. 7-73)

U.S. DEPT. OF COMM. BIBLIOGRAPHIC DATA SHEET	1. PUBLICATION OR REPORT NO. NBSIR 76-1031	2. Gov't Accession No.	3. Recipient's Accession No.

4. TITLE AND SUBTITLE

Shape Dependence of Light-Scattering Behavior of Dust Particles

5. Publication Date: June 1976

6. Performing Organization Code

7. AUTHOR(S)

R. Zerull

8. Performing Organ. Report No.

9. PERFORMING ORGANIZATION NAME AND ADDRESS

NATIONAL BUREAU OF STANDARDS
DEPARTMENT OF COMMERCE
WASHINGTON, D.C. 20234

10. Project/Task/Work Unit No. 4928677

11. Contract/Grant No.

12. Sponsoring Organization Name and Complete Address (*Street, City, State, ZIP*)

same as No. 9

13. Type of Report & Period Covered: Final Report

14. Sponsoring Agency Code

15. SUPPLEMENTARY NOTES

16. ABSTRACT (*A 200-word or less factual summary of most significant information. If document includes a significant bibliography or literature survey, mention it here.*)

The most important characteristic which determines the light-scattering behavior of particles is their size distribution, their concentration, their shape, and their material composition. This paper concerns itself with the measurement of the effects of shape on light-scattering behavior. Only a few shapes have been appropriately modeled and if the shape dependence can be determined, the remaining characteristics pose no special difficulties.

17. KEY WORDS (*six to twelve entries; alphabetical order, capitalize only the first letter of the first key word unless a proper name; separated by semicolons*)

Aerosols; dusts; light-scattering; Mie theory; particles; Rayleigh scattering.

18. AVAILABILITY

[XX] Unlimited

[ ] For Official Distribution. Do Not Release to NTIS

[ ] Order From Sup. of Doc., U.S. Government Printing Office Washington, D.C. 20402, SD Cat. No. C13

[XX] Order From National Technical Information Service (NTIS) Springfield, Virginia 22151

19. SECURITY CLASS (THIS REPORT)	21. NO. OF PAGES
UNCLASSIFIED	22
20. SECURITY CLASS (THIS PAGE)	22. Price
UNCLASSIFIED	$3.50